Structural and magnetic behavior of Ar+implanted Co/Pd multilayers: Interfacial mixing

L. F. Schelp, M. Carara, A. D. C. Viegas, M. A. Z. Vasconcellos, and J. E. Schmidt

Structural and magnetic behavior of Ar⁺-implanted Co/Pd multilayers: Interfacial mixing

L. F. Schelp, M. Carara, A. D. C. Viegas, M. A. Z. Vasconcellos, and J. E. Schmidt
Instituto de Física, Universidade Federal do Rio Grande do Sul, CP-15051, 91501-970,
Porto Alegre, RS, Brazil

The magnetization behavior of Co/Pd multilayers has been analyzed as a function of the degree of interfacial mixing among the Co and Pd layers. Controlled atomic mixing was induced by low-dose and low-flux ion implantation and a follow-up of the structural status of the samples was made by simulation of the high-angle x-ray-diffraction data. Values of the saturation magnetization as a function of the broadness of Co concentration profile are presented and explained by a simple model based on the parameters obtained from the x-ray simulations.

I. INTRODUCTION

In the last decade Co/Pd multilayers (MLs) have been one of the most extensively studied systems in the field of nanostructured magnetic materials. The interest stems mainly from the perpendicular magnetic easy axis observed in samples with few atomic Co layers, which could qualify these systems for technological applications as high-density magnetic recording media.[1-3] Although much is known about the Co/Pd multilayer system, there is a considerable lack of knowledge about the relationships between the saturation magnetization M_s and interface characteristics such as coherency, roughness, and intermixing.

Reported results on sharp interface Co/Pd MLs have shown that M_s (per Co volume) is larger than in bulk Co, increasing with the number of Pd monolayers until a maximum is reached.[4,5] Polarization of Pd atoms and other magnetic interactions have been claimed to explain this behavior.[6,7] As long as the possibility of intermixing is considered, a recent result[8] has indicated that the M_s value decreases as the interface gets more diffuse. Since in real samples the interface features depend on the method and parameters of deposition, comparison between different M_s data is meaningful only if a detailed structural characterization of the interface is done.

In this work the effect of Ar⁺-ion implantation on MLs of Co/Pd has been studied in terms of induced structural and magnetic modifications. Controlled atomic mixing at the interfaces was forced by low-dose and low-flux radiation and a follow-up of the structural status of the samples was made by measurement and simulation of the high-angle x-ray diffraction (XRD). The effect of the interface mixing on the magnetization was also studied, and the analysis was based on a simple model using the parameters of the Co concentration profiles, as obtained from XRD simulations.

II. EXPERIMENTAL DETAILS

The MLs were deposited on Si wafers by means of two electron-beam guns. The pressure before the deposition was 1×10^{-8} mbar. Rates of deposition were controlled and maintained by a quartz-crystal oscillator close to 1 Å/s. The samples were produced in two different batches of 18 bilayers with nominal thicknesses of 12 and 45 Å for Co and Pd layers, respectively.

Each set of samples was submitted to 230 keV of Ar⁺ bombardment, maintaining the substrate at room temperature in one case, and at 77 K in the other. The energy of the beam was chosen [as determined from TRIM 89-ZBL (Refs. 9 and 10)], in order to guarantee that the maximum of energy deposition was in the middle of the ML (it corresponds to 80% of the projected range[11]). The current density was low enough (50 nA/cm²) to avoid sample heating and doses were used in the range of 1×10^{13} up to 5×10^{14} ions/cm².

The XRD were obtained using the CuKα radiation, with incident and diffracted beams in a plane normal to the film surface. Due to its sensitivity to refractive effects and to errors introduced by a possible incorrect positioning of the samples at the goniometer center (in the used configuration), diffractograms in the small angle region are used just to check qualitatively the results obtained in the high-angle region.

The room-temperature magnetic measurements were performed using a vibrating sample magnetometer.

III. X-RAY CHARACTERIZATION AND SIMULATIONS

The patterns of the as-deposited (AD) samples show at least three sharp peaks in the low-angle region (between 1° and 8°) and up to four satellites visible around the main peak near the Pd(111) diffraction position [see Fig. 1(a)]. Due to the low thickness of Co layers, the Co(002) or (111) peaks are small or invisible as usual for this kind of system. From these general x-ray features we conclude that the samples present chemical modulation with highly (111)-textured Pd. The period Λ of the MLs, extracted from the relative position of the peaks in the high-angle region, were 68 and 63 Å for the first and second batch, respectively, as is discussed below.

Additional information on the structural characteristics of the MLs can be extracted by means of high-angle spectra simulation, applying a one-dimensional kinematics approximation. A number of different models have been created and a complete review about this issue can be found.[12]
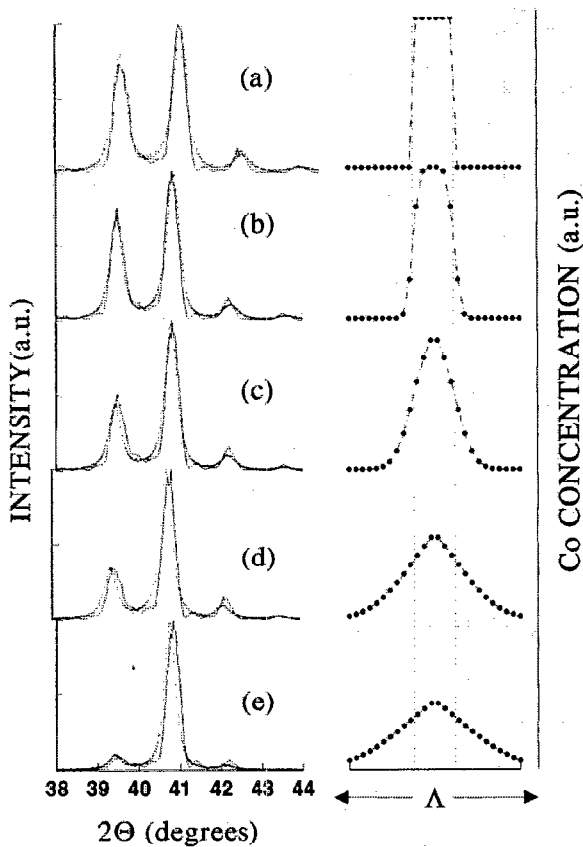
FIG. 1. Left-hand side: Experimental (dots) and simulated (line) XRD for a Co/Pd for different doses implanted at room temperature. The doses were (a) 0, (b) 1×10^{13}, (c) 5×10^{13}, (d) 1×10^{14}, (e) 5×10^{14} ions/cm^2. The fixed parameters used in the simulation were $d_{Co} = 2.035$ Å, $d_{Pd} = 2.246$ Å, $\bar{n}_{Co} = 6$, $\bar{n}_{Pd} = 25.3$, $L = 270$ Å, $\rho_{Co}/\rho_{Pd} = 1$, and Debye–Waller factors of 0.27 and 0.36 for Co and Pd, respectively. The values of Γ were (a) 0.1, (b) 1.1, (c) 3.2, (d) 4.2, and (e) 10. Right-hand side: the Co concentration profiles related to each Γ value for one period Λ.

In our simulation it was considered that, for a ML with N bilayers (of $n_{Co}^j + n_{Pd}^j$ monoatomic layers of Co and Pd in the jth bilayer, $j = 1-N$), we can evaluate the amplitude of diffraction $A(q)$ by adding the contributions from the first to the last atomic monolayer, that is

$$A(q) = \sum_{i=1}^{k} W_i f_i(q) e^{i\pi q x_i}, \tag{1}$$

where q is the diffraction vector $[q = (4 \sin \theta)/\lambda]$, W_i is a Debye–Waller parameter, $f_i(q)$ is the scattering factor multiplied by the number of atoms per unit area, and x_i is the position of the ith atomic layer. The total number of monolayers in the sample is given by k. For an ideal ML (without grains, with perfectly sharp interfaces and with the very same thicknesses for Co and Pd layers throughout the whole ML), the values assumed by $f(q)$ and W in the ith atomic layer will be those expected for bulk Co and Pd. The position of each plane is determined adding the bulk atomic parameters d_{Co} and d_{Pd} (corresponding to one specific crystal orientation) from the substrate to the top of the ML film.

While dealing with real samples with grains, interface alloy formation, and variations in the number of monoatomic

layers n_{Co}^j and n_{Pd}^j for each bilayer j, we have considered changes in the parameters as described as follows.

(i) Bilayer thicknesses: Considering that each layer (of Co and Pd) does not necessarily have an equal number of atomic planes for different bilayers j, we use for n_{Co}^j and n_{Pd}^j integer numbers extracted from two discrete pseudorandomic Gaussian distributions, centered at averages $\bar{n}_{Co}$ and $\bar{n}_{Pd}$ (not necessarily integer numbers anymore), with half-full-width intensity determined by σ_a by means of $\exp(n_a - \bar{n}_a/\sigma_a)^2$, where $a = $ Co or Pd.

(ii) Grains: To simulate the effect of limited dimension of the regions that scatter coherently (as actually occurs in polycrystalline samples) we introduced a random increment to the x variable whenever a predetermined adjustable parameter L is reached. Its purpose is to cause the loss of coherence in the phase of the scattering amplitude and so L is related to the coherent length normal to the film plane.

(iii) Interface intermixing: in order to contemplate interdiffusion at the interfaces, we use a Co concentration profile of the form[13]

$$C_{Co}(i) = B[1 + \text{erf}(i/\Gamma)]/2 \tag{2}$$

from the middle of one Pd layer to the center of the nearest Co layer, where B is a normalization constant introduced to guarantee the conservation of mass, and the parameter Γ is related to the broadness of the Co concentration profile. As a first approximation, we assumed that the atomic distances d_{Co} and d_{Pd} (within the diffused region) should vary following a function similar to the Co concentration profile (Vergard's law). This assumption seems to be reasonable for miscible alloy systems such as Co-Pd, and it was also used to calculate $f(q)$ and the Debye–Waller parameters for each atomic plane.

The basic characteristics of the calculated spectra and their relation to the parameters used, are similar to those observed in XRD simulations of other systems.[14] The period of the bilayers determines the angular distance between peaks, while $\bar{n}_{Co}/\bar{n}_{Pd}$ control the main peak position. The width of the peaks is mainly related to the coherence length L, while σ_{Co} and σ_{Pd} allow the fitting of the background between the peaks. The intensities of the satellite peaks relative to the main one are determined from the broadness of Co concentration profile Γ. We find that different parameters are related to different features of experimental spectra and can be chosen one by one, independently (with little interference among them).

IV. RESULTS AND DISCUSSION

A. Structure

In the left-hand side of Fig. 1, the experimental and simulated high-angle XRD for the AD and implanted samples are presented.

The values of $\bar{n}_{Co}$ and $\bar{n}_{Pd}$ [Fig. 1(a)] show that the difference between the nominal and measured values of Λ is mainly due to the variation of the Pd layer thickness (~15% greater than the nominal values). The value of Γ required to fit this spectrum is near zero corresponding to an almost atomically sharp interface. The Co concentration profile aris-

ing from each Γ parameter is shown in the right-hand side of Fig. 1, for one Λ. Items (b), (c), (d), and (e) in Fig. 1 show that the main modification in the spectra of the implanted MLs is a decrease at the intensity of the satellite peaks with increasing doses.

For doses up to 5×10^{13} the experimental spectra can be well simulated changing only the intermixing parameter Γ. All other parameters were maintained constant and equal to those used in the AD simulations. This option is reasonable for parameters such as $\bar{n}_{Co}$, $\bar{n}_{Pd}$, σ_{Co}, and σ_{Pd}. Some doubt could arise while fixing the value of grain size L, because increases of up to 50% in coherence length have been observed in MLs under similar bombardment conditions.[15] However, as can be seen from the width of the experimental peaks in Fig. 1, the coherence lengths increase, for all samples, is less than 15%. No noticeable influence on the Γ parameter was found simulating the XRD with L 15% greater than the value used in the AD fittings with $L = 270$ Å. The values of grain size obtained from scanning tunneling microscopy measurements from the surface of the AD sample were around 300 Å.[16]

For doses above 1×10^{14} ions/cm², the peaks of the experimental spectra present a slight shift towards small angles. This shift corresponds to an increase of about 2 Å in the period of the ML and, in a first approach, could be attributed to ion-implanted inclusions. This hypothesis can be discarded in view of the low doses used (one monolayer corresponds to 1×10^{15} atoms/cm²). We attributed this shift to voids produced by the implantation which implies in a reduced mass density. This should be followed by a progressive loss of texture in the sample as suggested by the broadening in the Co concentration profiles of Figs. 1(d) and 1(e). Since texture is essential in performing the calculation of the diffraction spectrum, the values of Γ extracted from XRD simulations at these high doses must be taken with caution.

The analysis of the results indicates that local interdiffusion at the interfaces is the main effect induced by ion implantation with doses lower than 1×10^{14} ions/cm² (in opposition to thermal treated Co/Pd MLs where the interdiffusion through grain boundaries plays a more important role[17]). In the present experimental conditions, doses greater than 1×10^{14} impose degrees of disorder that prejudice a quantification of the interface mixing by XRD in view of the loss texture.

Interfacial mixing can be understood in the scope of ion beam mixing (IM) models, i.e., collisional mixing[18,19] and thermal spike diffusion.[19,20] The last model takes into account the chemical nature of the elements and has been more successful in describing IM processes. In the low-temperature limit, IM is temperature independent and the energy imparted by the primary ion to the lattice generates atomic relocations in a cascade of nuclear collisions. The effect of higher doses is to induce atomic relocations over extended regions of the ML system as a consequence of a spatial superposition of collision cascade or subcascades.

In the low-flux and -dose limits, when there is no temporal and spatial cascade superposition, Γ averages mixing over the whole sample. For higher doses, the spatial depth distribution of cascade collision is more peaked at the central
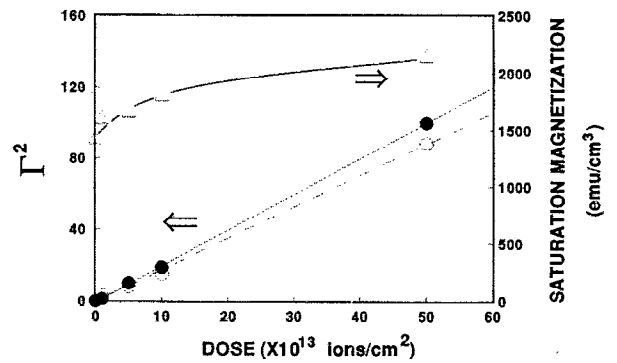

FIG. 2. (Δ) M_s and Γ parameter (determined by XRD simulations) as a function of ion dose for samples implanted at (○) 77 K and (●) room temperature.

part of the ML. In this regime, superposition of new cascades in a volume previously modified induces less effective mixing in the middle than the external regions of the ML. Also, the interpretation of Γ should no longer be a simple average over all the sample, since now two different effects are being induced by ion irradiation.

Figure 2 shows the Γ values extracted from the simulation as a function of the dose for samples implanted at different temperatures. The observed behavior agrees with that expected from collisional or thermal spike mixing models, i.e., a linear dependence between dose and Γ^2. The mixing efficiency, given by the slope of the straight line in Fig. 2, is higher for irradiation at 300 K than at 77 K, since in the first case radiation-enhanced diffusion effects must be taken into account.

B. Saturation magnetization

Figure 2 also shows M_s measured at room temperature for samples submitted to different doses. The results show that the magnetization of the samples grows with the implanted dose. We have related this behavior to the degree of interfacial mixing and dismissed any other possible mechanism related to structural modification as responsible for these changes.

While Co and Pd mix at the interfaces, two opposite effects will be simultaneously present: (i) the number of Pd atoms polarized by nearest Co increases, increasing the measured M_s; and (ii) the portions of the material with low Co concentration increase, thus decreasing the magnetic moment at room temperature of the samples. This effect is related to the Curie temperature T_c, which is below room temperature for CoPd alloys with less than 10 at.% Co. The M_s presented in Fig. 2 is a clear indication that in our samples the former mechanism prevails.

A better understanding of the diffusion effect on magnetization can be obtained with a very simple model, where the final magnetization is evaluated summing up the contributions of all layers, or simply
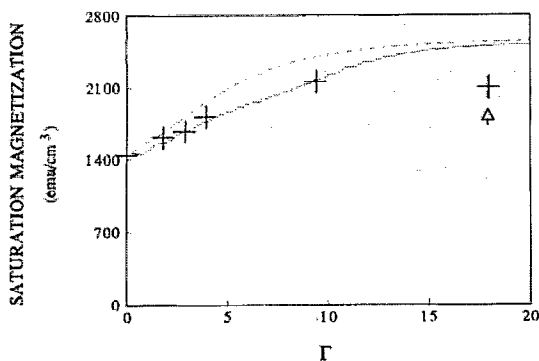
FIG. 3. Experimental values of M_s as a function of Γ (crosses). Calculated M_s values with (solid line) and without (dashed line) the cutoff condition. The signed experimental value corresponds to a dose of 1×10^{15} Ar$^+$/cm^2.

$$M_s = \sum_{i=1}^{k} m_i(\bar{C}_{Co})\rho_i, \qquad (3)$$

where ρ_i is the number of atoms per area in the ith plane, and C_{Co} is obtained using Eq. (2) and

$$\bar{C}_{Co}(i) = \frac{C_{Co}(i-1) + C_{Co}(i) + C_{Co}(i+1)}{3}. \qquad (4)$$

In Eq. (3), $m_i(C_{Co})$ is the room-temperature average magnetic moment (as obtained from the data of CoPd alloys[21]) related to the cobalt concentration per plane (as extracted from the XRD). Since we do not have the means of obtaining detailed information on the magnetic status of the individual atoms within the material, we overcome this limitation by computing the relative concentration for the ith monolayer considering adjacent planes [Eq. (4)]. In this way we take into account the effect of the nearest-neighbor planes.

The results of the M_s calculations, for different degrees of intermixing, are presented in Fig. 3 (dashed line), together with the experimental values (crosses). The M_s value of the AD samples was adjusted with a number of Co atoms per unit area 12% lower than the value expected from the bulk densities, which can be related to voids and defects in the ML.

The difference between the data and the model can in part be explained if one realizes that, according to the CoPd magnetic phase diagram, at room temperature, no magnetic order is expected in the alloys with low Co concentration. Introducing a cutoff condition to take out contributions from regions where the Co concentration is less than 10%, a decreasing M_s value can be calculated for samples with very thin Co layers (in comparison to Pd ones), in accordance with other experimental result.[8] For our thicknesses the calculated M_s still increases but a better adjustment is achieved in the low Γ range. The introduction of this abrupt cutoff condition imposes discontinuities in the obtained curve (Fig. 3, line).

The remaining disagreement in the high Γ range could in part be due by the nonuniform concentration profile of the implanted ions throughout the samples. The high density of

defects in the central portion of the ML, in the high-dose range, produces loss of texture imposing higher error in the determination of Γ.

V. CONCLUSIONS

We have followed the structural and magnetic evolution of (111) Co/Pd MLs submitted to Ar$^+$ implantation through XRD characterization and magnetization measurements.

The results show that the evolution of XRD spectra for doses lower than 1×10^{14} Ar$^+$/cm^2 can be adjusted changing only the parameter that quantifies the average broadness of the concentration profile of Co at the interfaces of the ML. These same concentration profiles were used as starting points to calculations that explain the general behavior of the M_s while the intermixing grows.

Ion implantation has been proved to be a useful technique to induce step-by-step modifications in thin films. Small modification at the interfaces of a ML with thin periods (lower than 70 Å in our work) was visible by XRD technique in a range of doses normally not possible by techniques generally used to quantify ion-beam mixing. Rutherford backscattering and Auger spectroscopy, for example, require higher doses of implantation and thicker layers.

Room-temperature M_s measurements are sensitive to small degrees of interfacial mixing, indicating that alloying at the interface has to be taken into account for a better understanding of the magnetization in Co/Pd MLs. A cutoff condition has also to be introduced to account for the reduction of M_s due to low-T_c portions of the ML. Our results indicate that the dominating effect depends on the thickness range used in each layer. In MLs with the thicknesses used in this work, as also observed in annealed Co/Pd MLs,[22] the polarization of Pd prevails over other possible Co-Pd or Co-Co interactions, and an increasing in M_s is observed.

[1] P. F. Carcia, A. D. Meinhaldt, and A. Suna, Appl. Phys. Lett. **47**, 178 (1985).
[2] S. Hashimoto, Y. Ochiai, and K. Aso, J. Appl. Phys. **66**, 4909 (1989).
[3] J. V. Haezer, B. Hillebrands, R. L. Stamps, G. Güntherodt, C. D. England, and C. M. Falco, J. Appl. Phys. **69**, 2448 (1991).
[4] D. G. Stinson and S.-C. Shin, J. Appl. Phys. **67**, 4459 (1990).
[5] H. J. G. Draaisma, W. J. M. de Jonge, and F. J. A. den Broeder, J. Magn. Magn. Mater. **66**, 351 (1987).
[6] R. H. Victora and J. M. Maclaren, J. Appl. Phys. **69**, 5652 (1991).
[7] K. Miura, H. Kimura, S. Imanaga, and Y. Hayafuji, J. Appl. Phys. **72**, 4826 (1992).
[8] P. He, Z.-S. Shan, J. A. Woollam, and D. J. Sellmyer (unpublished).
[9] J. F. Ziegler, J. P. Biersack and U. Littmark, *The Stopping and Range of Ions in Solids* (Pergamon, New York, 1985), Vol. 2.
[10] J. F. Ziegler, J. P. Biersack, U. Littmark, *The Stopping and Range of Ions in Solids* (Pergamon, Oxford, 1984).
[11] K. B. Winterbon, P. Sigmund, and J. B. Sanders, Mat. Fys. Medd. Dan. Vid. Selsk. **37**, 1 (1970).

[12] E. E. Fullerton, I. K. Schuller, H. Vanderstraeten, and Y. Bruynseraede, Phys. Rev. B **45**, 9292 (1992).

[13] M. A. Z. Vasconcellos, J. A. T. Borges da Costa, W. Schreiner, and I. J. R. Baumvol, Appl. Phys. Lett. **55**, 513 (1989).

[14] M. B. Stearns, C. H. Lee, and T. L. Groy, Phys. Rev. B **40**, 8256 (1989).

[15] H. A. Atwater, C. V. Thompson, and H. I. Smith, J. Appl. Phys. **64**, 2337 (1988).

[16] Digital Instruments Inc. (private communication).

[17] A. D. C. Viegas, L. F. Schelp, M. Carara, and J. E. Schmidt (unpublished).

[18] W. L. Johnson, Y. T. Cheng, M. Van Rossum, and M.-A. Nicolet, Nucl. Instrum. Methods B **7/8**, 657 (1985).

[19] M. A. Z. Vasconcellos, J. A. T. Borges da Costa, W. Schreiner, and I. J. R. Baumvol, Phys. Status Solidi A **122**, 105 (1989).

[20] P. Sigmund and A. Gras-Marti, Nucl. Instrum. Methods **182-183**, 25 (1981).

[21] R. M. Bozorth, P. A. Wolff, D. D. Davis, V. B. Compton, and J. H. Wernick, Phys. Rev. **122**, 1157 (1961).

[22] N. Sato, J. Appl. Phys. **64**, 6424 (1988).

5266   J. Appl. Phys., Vol. 75, No. 10, 15 May 1994

Schelp *et al.*